JURNAL TEKNOLOGI TERPADU VOL.14 NO. 1 APRIL 2026 ISSN 2338 - 6649

Received: Januari 2026	Accepted: Maret 2026	Published: April 2026

Commutation Performance Enhancement of Sensorless BLDC Motor Using Finite Impulse Response Filtering in Back-EMF Detection

Ony Asrarul Qudsi[1*], Era Purwanto[2], Sulis Wanto[3], Muhammad Rizani Rusli[4]

[1,2,3,4] *Department of Electrical Engineering, Politeknik Elektronika Negeri Surabaya, Indonesia*

[*]*Email: ony@pens.ac.id*

Abstract

Sensorless Brushless Direct Current (BLDC) motors are widely used in industrial applications due to their high efficiency and low maintenance requirements. However, commutation based on Back-Electromotive Force (Back-EMF) zero-crossing detection is highly susceptible to noise, leading to commutation timing inaccuracies. This paper proposes an improvement in sensorless BLDC motor commutation performance through the application of a Finite Impulse Response (FIR) digital filter to the Back-EMF detection signal. The FIR filter is designed to attenuate high-frequency harmonic components without compromising system stability. The proposed method is implemented on a three-phase inverter system employing six-step commutation controlled by a microcontroller. Simulation results indicate that the dominant noise frequency in the Back-EMF signal is reduced from 347.6 Hz to 212.5 Hz after filtering. Furthermore, hardware experimental results demonstrate a reduction in disturbance frequency from 317.23 Hz to 265.43 Hz. The application of the FIR filter improves the reliability of zero-crossing detection and enhances commutation timing accuracy compared to an unfiltered system. These results confirm that the proposed approach is effective in improving the commutation performance of sensorless BLDC motors based on Back-EMF detection.

Keywords: Sensorless BLDC motor, Back-EMF zero-crossing detection, Finite Impulse Response (FIR) filter, six-step commutation

1. Introduction

Sensorless Brushless Direct Current (BLDC) motors are widely employed in industrial applications, electric vehicles, and automation systems due to their high efficiency, high power density, and low maintenance requirements. In sensorless operation, rotor position estimation based on Back-Electromotive Force (Back-EMF) zero-crossing detection is a commonly adopted approach because of its simple structure and the elimination of additional mechanical sensors [1], [2]. However, this method suffers from significant challenges arising from noise and harmonic distortion in the Back-EMF signal, particularly at low speeds and under transient operating conditions. These disturbances lead to commutation timing inaccuracies, which directly degrade motor performance, increase torque ripple, and reduce overall system efficiency [3].

Various methods have been developed to improve the reliability of Back-EMF zero-crossing detection [4]. Analog filter-based approaches, such as RC and LC low-pass filters, are relatively simple to implement. However, they suffer from limited flexibility and non-constant phase-shift characteristics [5]-[7]. Digital Infinite Impulse Response (IIR) filtering methods offer lower computational complexity, but they may introduce potential instability due to the presence of poles in the system [9], [10]. Other approaches, including model-based observers and mathematical transformation techniques, are capable of enhancing detection accuracy. Nevertheless, they require precise motor parameters and involve higher computational complexity,

making them less suitable for embedded systems with limited computational resources [11]–[14].

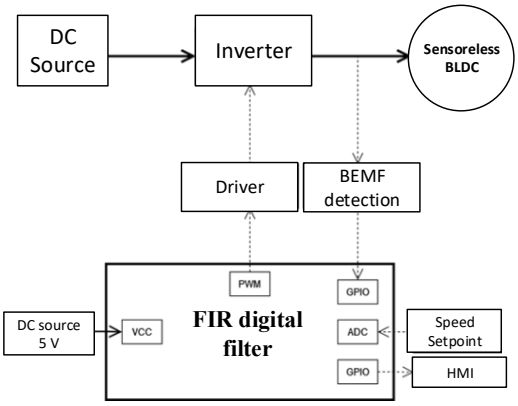

Figure 1. System Block Diagram

This paper proposes the application of a Finite Impulse Response (FIR) digital filter to the Back-EMF detection signal in order to enhance the commutation performance of sensorless BLDC motors, as illustrated in Figure 1. The FIR filter is selected due to its intrinsic stability, linear phase response, and its ability to attenuate high-frequency harmonic components without compromising system stability [15]-[19]. The proposed method is implemented on a three-phase inverter system employing microcontroller-based six-step commutation, thereby preserving a simple and practical control structure suitable for embedded applications.

The main contributions of this work are summarized as follows:

1. The design and implementation of a digital FIR filter for Back-EMF signal processing in a sensorless BLDC motor system.
2. A quantitative evaluation of the effect of FIR filtering on noise reduction and the improvement of zero-crossing detection reliability through both simulation and hardware experiments.
3. The demonstration of enhanced commutation timing accuracy compared with an unfiltered system, while maintaining low system complexity suitable for industrial applications.

Based on the problems and approaches described above, this paper is organized as follows. Section II presents the modeling of the sensorless BLDC motor, the Back-EMF zero-crossing detection method, and the relevant characteristics of the digital FIR filter. Section III describes the proposed method, including the FIR filter design and its implementation in a three-phase inverter system with six-step commutation. Section IV presents the simulation and hardware experimental results along with the corresponding performance analysis. Finally, Section V concludes the paper and outlines directions for future research aimed at further improving the performance of sensorless BLDC motor systems.

2. System Modelling

The sensorless Brushless Direct Current (BLDC) motor considered in this study is modeled as a three-phase system based on an equivalent circuit approach to accurately represent the electrical and electromechanical characteristics of the motor. The model is developed under several key assumptions as follows. First, the BLDC motor is assumed to have a three-phase star-connected (Y-connection) configuration without direct access to the physical neutral point; therefore, the neutral voltage is obtained through the formation of a virtual neutral point derived from the combination of the three phase voltages. Second, each motor phase is assumed to have identical electrical parameters, namely the stator resistance R_s and self-inductance L_s, while mutual inductances between phases are neglected or assumed to be incorporated into an equivalent inductance value. This assumption is adopted to simplify the model while preserving the dominant dynamic characteristics of the motor.

Third, the Back-Electromotive Force (Back-EMF) is modeled as a trapezoidal function that depends on the electrical rotor position θ_e and the electrical angular velocity ω_e. This Back-EMF representation is consistent with the physical characteristics of BLDC motors employing non-sinusoidal permanent

magnet flux distribution. Fourth, the motor drive system is modeled using a three-phase inverter represented by switching functions that generate equivalent phase voltages as inputs to the motor model. These phase voltages are determined based on the switching states of the inverter under the six-step commutation scheme.

Based on these assumptions, the BLDC motor model provides a mathematical representation of the relationship among inverter input voltages, stator phase currents, and Back-EMF voltages. This model serves as the foundation for zero-crossing detection analysis and for evaluating the effect of FIR filtering on commutation performance. Furthermore, the model enables systematic analysis of noise effects on the Back-EMF signal and facilitates assessment of the effectiveness of the proposed filtering method.

2.1. BLDC Modelling

Under normal operating conditions with six-step commutation, only two phases conduct current simultaneously, while the remaining phase operates in a floating state. The Back-EMF voltage of this floating phase is exploited to estimate the rotor position. Figure 2 depicts the single-phase equivalent circuit model of the BLDC motor, consisting of the stator resistance R_s, stator inductance L_s, and the Back-EMF source E. This model is employed to describe the relationship among the applied phase voltage, the phase current, and the Back-EMF voltage, which is inherently dependent on the rotor speed.

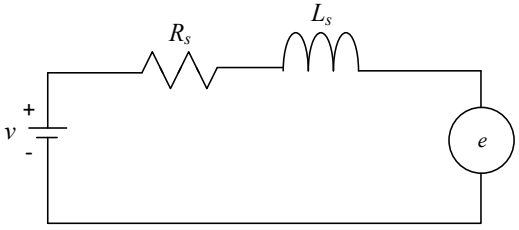

Figure 2. Equivalent Circuit of the BLDC Motor

The phase voltage equations are expressed as:

$$\begin{cases} v_a = R_s i_a + L_s \dfrac{di_b}{dt} + e_b \\ v_b = R_s i_b + L_s \dfrac{di_c}{dt} + e_a \\ v_c = R_s i_c + L_s \dfrac{di_c}{dt} + e_c \end{cases} \quad (1)$$

Since the sensorless BLDC motor is star-connected without a physical neutral point, it follows that:

$$i_a + i_b + i_c = 0 \quad (2)$$

Therefore, only two phase currents are considered as independent state variables, as expressed by the following equation:

$$x_e = \begin{bmatrix} i_a \\ i_a \end{bmatrix}, i_c = -i_a - i_b \quad (3)$$

Accordingly, the state-space model of the BLDC motor can be expressed as:

$$\begin{cases} \dot{x}_e = A_e x_e + B_e (v_{ab} - e_{ab}) \\ A_e = -\dfrac{R_s}{L_s} I_2 ; B_e = -\dfrac{1}{L_s} I_2 \end{cases} \quad (4)$$

Where I_2 denotes the 2x2 identity matrix.

2.2. Back-EMF Zero-Crossing Detection Modeling

Back-EMF zero-crossing detection is performed by comparing the voltage of the floating phase with a virtual neutral point derived from the combination of the three motor phases. A zero-crossing event occurs when the Back-EMF voltage of the floating phase intersects the neutral reference voltage, which ideally corresponds to the rotor position at every 60 electrical degrees. In practical implementations, however, the Back-EMF signal is contaminated by inverter switching noise and high-frequency harmonics, thereby necessitating appropriate signal processing prior to the comparison stage.

The Back-EMF is modeled as a normalized trapezoidal waveform function $f(\cdot)$ with respect to the electrical rotor position θ_e.

$$\begin{cases} e_a = K_e \omega_e f(\theta_e) \\ e_b = K_e \omega_e f(\theta_e - \frac{2\pi}{3}) \\ e_b = K_e \omega_e f(\theta_e + \frac{2\pi}{3}) \end{cases} \quad (5)$$

With $\omega_e = p.\omega_m$, where p denotes the number of pole pairs and ω_m represents the mechanical angular speed. The trapezoidal function $f(\theta)$ can be expressed as a 2π periodic function.

2.3. Digital FIR Filter Modelling

The FIR filter is designed as a low-pass filter to attenuate high-frequency harmonic components without introducing system instability. The linear-phase characteristic of the FIR filter ensures that no significant time distortion is imposed on the zero-crossing signal, thereby preserving commutation timing accuracy. To enhance the quality of the Back-EMF signal, a Finite Impulse Response (FIR) digital filter is employed and modeled as a linear time-invariant system. The output of the FIR filter is expressed as follows:

$$y_f[n] = \sum_{k=0}^{N-1} h_k y[n-k] \quad (6)$$

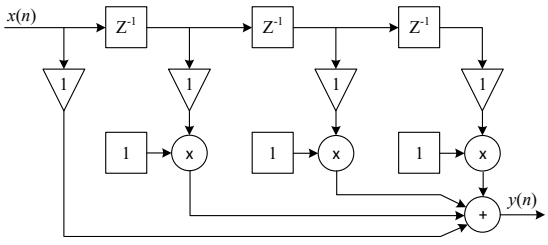

Figure 3. Structure of the Digital FIR Filter

Figure 3 illustrates the structure of the digital FIR filter, which consists of a cascade of one-sample delay elements (Z^{-1}), coefficient multipliers, and summation blocks. Each Z^{-1} block stores a previous sample of the input signal, while the multiplier blocks represent the FIR filter coefficients, and all weighted samples are summed to produce the filter output. Let $x(n)$ denote the input Back-EMF signal, h_k the FIR filter coefficients, N the filter order, and $y(n)$ the filtered output signal. Accordingly, the input–output relationship of the FIR filter can be expressed in state-space form as follows:

$$x_f[n] = \begin{bmatrix} y[n-1] \\ y[n-2] \\ \vdots \\ y[n-(N-1)] \end{bmatrix} \quad (7)$$

So,

$$\begin{cases} x_f[n+1] = A_f x_f[n] + B_f y[n] \\ y_f[n] = C_f x_f[n] + D_f y[n] \end{cases} \quad (8)$$

Where,

$$A_f = \begin{bmatrix} 0 & 0 & \cdots & 0 \\ 1 & 0 & \cdots & 0 \\ 0 & 1 & \ddots & 0 \\ \vdots & \ddots & \ddots & 0 \end{bmatrix}; B_f = \begin{bmatrix} 1 \\ 0 \\ \vdots \\ 0 \end{bmatrix} \quad (9)$$

$$C_f = \begin{bmatrix} h_1 & h_2 & \cdots & h_{N-1} \end{bmatrix}; D_f = h_0$$

2.4. Proposed Method

The FIR filter is inserted into the Back-EMF signal processing path to suppress high-frequency components caused by inverter switching and harmonics, thereby making zero-crossing events more stable and repeatable in both simulation and hardware implementations. The flowchart in Figure 4 depicts the stages of the proposed algorithm for sensorless BLDC motor commutation based on FIR-assisted Back-EMF signal processing. The procedure begins with system initialization, including the configuration of three-phase PWM, timers, ADC or comparator modules, initialization of FIR filter coefficients, sample buffers, and the initial commutation state. In each control cycle, the system selects the phase that is currently in the floating condition according to the active commutation sector and acquires the detection signal $y[n]=v_x[n]-v_n[n]$. This signal is then processed by the FIR filter to attenuate high-

frequency noise components, yielding the filtered signal $y_f[n]$.

Subsequently, zero-crossing detection is performed based on the sign change or comparator output of $y_f[n]$. When a valid zero-crossing event is identified, the system computes the next commutation instant by applying a fixed delay derived from the estimated signal period, and then updates the commutation sector of the three-phase inverter. This cycle is continuously repeated while the system remains active, enabling more accurate and reliable commutation in sensorless BLDC motor control based on Back-EMF.

Subsequently, zero-crossing detection is performed based on the sign change or comparator output of $y_f[n]$. When a valid zero-crossing event is identified, the system computes the next commutation instant by applying a fixed delay derived from the estimated signal period, and then updates the commutation sector of the three-phase inverter. This cycle is continuously repeated while the system remains active, enabling more accurate and reliable commutation in sensorless BLDC motor control based on Back-EMF.

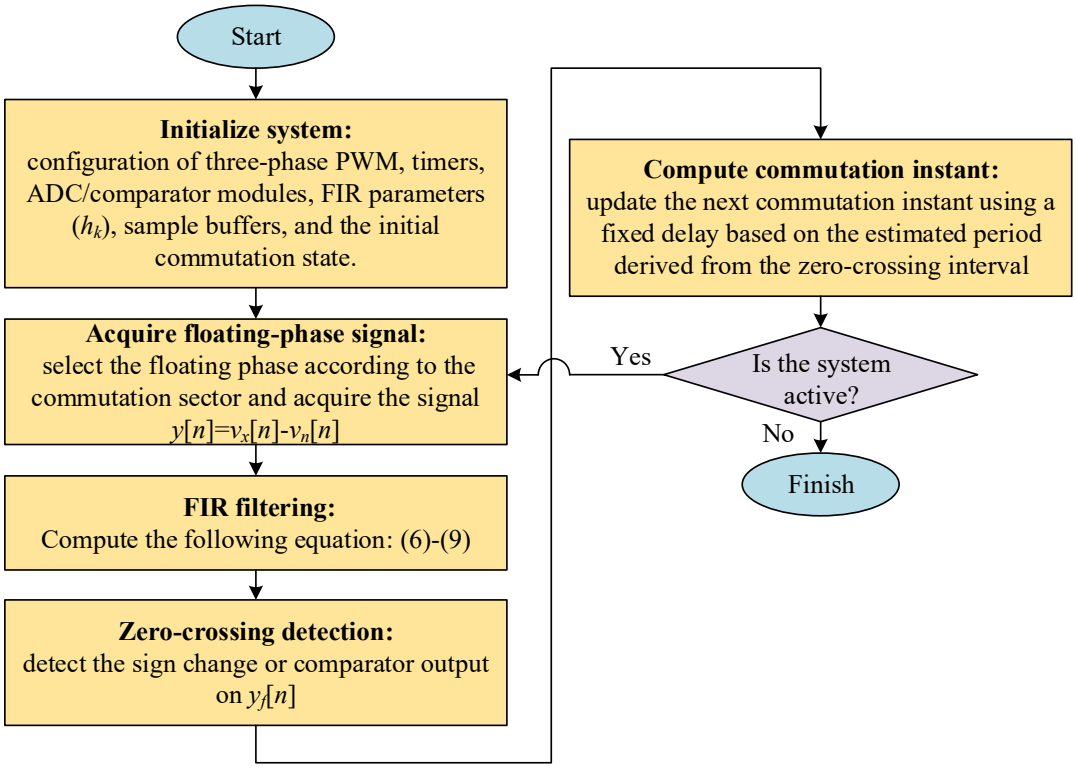

Figure 4. Flowchart of the Proposed FIR-Based Algorithm for Sensorless BLDC Commutation

The proposed method is implemented under two scenarios: integrated simulation to evaluate the effect of FIR filtering on the spectral and noise characteristics of the Back-EMF signal, and experimental validation on hardware to verify signal quality improvement in a real system subjected to inverter switching noise. In both scenarios, the observed system behavior focuses on the variation of the dominant disturbance components in the Back-EMF detection signal before and after FIR filtering, which is subsequently correlated with the stability of zero-crossing events and the accuracy of commutation timing.

3. Results and Analysis

3.1. Integrated Simulation

Integrated simulation is conducted to verify the performance of the proposed method prior to hardware implementation. The system model is developed in the MATLAB/Simulink environment and comprises a BLDC motor, a

three-phase inverter with six-step commutation, a Back-EMF detection circuit, and a digital FIR filter block. The simulation architecture is illustrated in Figure 5, which presents the overall system configuration in the simulation platform. In this study, the system operates under open-loop conditions to observe the characteristics of the Back-EMF signal and to evaluate the effect of FIR filtering on the zero-crossing detection process.

The simulation results indicate that the unfiltered Back-EMF signal still contains significant high-frequency noise components, as illustrated in Figure 6. After the signal is processed by the FIR filter, the waveform becomes smoother and more stable, with more clearly defined zero-crossing events, as shown in Figure 7. Spectral analysis further reveals that the dominant disturbance frequency in the detection signal is substantially reduced, from 347.6 Hz to 212.5 Hz after FIR filtering.

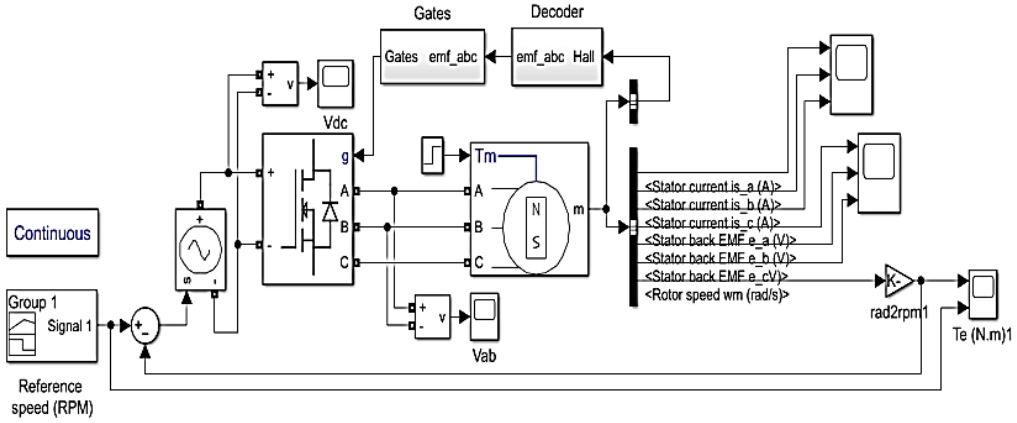

Figure 5. Main System in Integrated Simulation

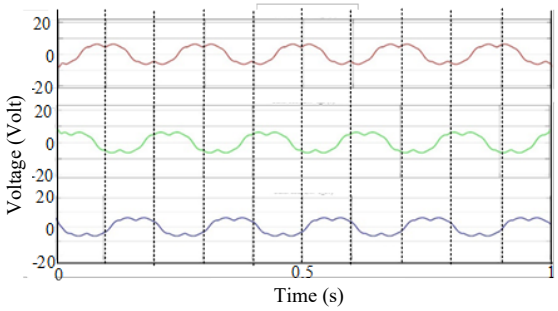

Figure 6. Back-EMF Voltage Signal Before FIR Filtering

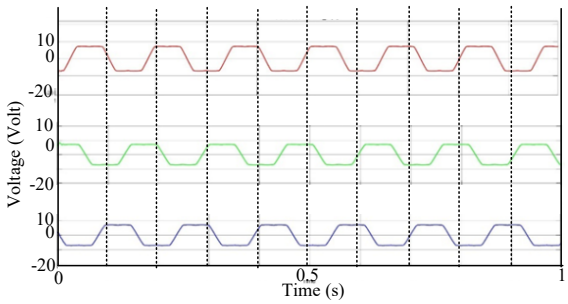

Figure 7. Back-EMF Voltage Signal After FIR Filtering

Figure 8 presents a comparison of the BLDC motor speed responses to the set point for the systems without and with FIR filtering under simulation. Both systems exhibit a rapid rise toward a steady-state speed of approximately 320-330 rpm. However, a clear distinction is observed during the initial transient phase. In the system without FIR filtering, the oscillation amplitude is larger and the damping is slower, indicating the influence of noise and inaccuracies in zero-crossing detection during the commutation process.

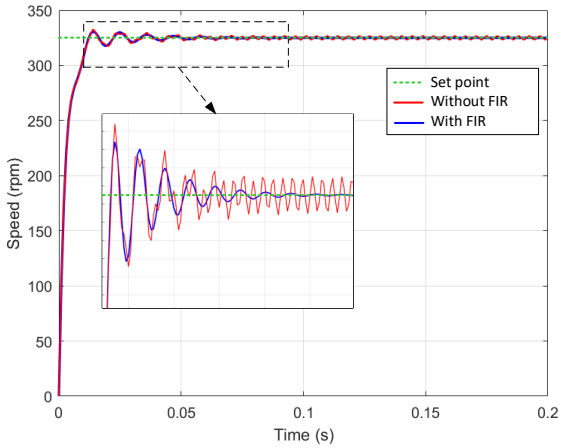

Figure 8. Comparison of BLDC Motor Speed Responses to the Set Point for Systems Without and With FIR Filtering in Simulation

In contrast, the system equipped with FIR filtering exhibits more heavily damped oscillations with smaller amplitudes and faster convergence to steady-state conditions. This behavior indicates that the FIR filter effectively suppresses speed ripple and transient fluctuations during startup, resulting in a smoother and more stable response. These results confirm that FIR-based filtering of the Back-EMF signal enhances the reliability of commutation detection and yields superior speed dynamics compared with the unfiltered system.

3.2. Experimental Validation

Experimental validation is conducted to ensure that the performance improvements observed in the simulation stage can also be realized in a real system. The experiments are carried out on a sensorless BLDC motor prototype driven by a three-phase inverter employing six-step commutation under open-loop operation. The system is evaluated under two configurations, namely without FIR filtering and with FIR filtering applied to the Back-EMF detection signal path. The hardware integration setup is illustrated in Figure 9.

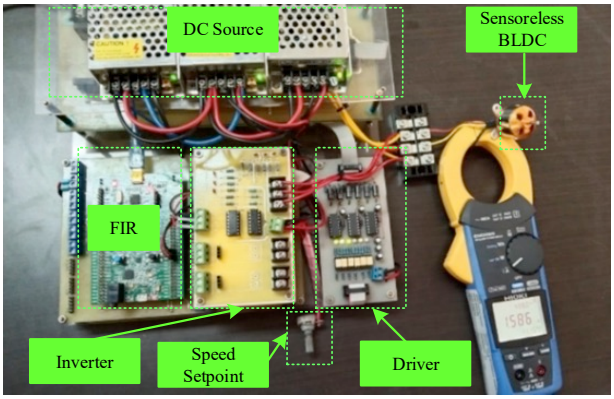

Figure 9. Hardware Integration for Experimental Setup

The experimental results demonstrate that the Back-EMF detection signal in the unfiltered system contains a higher level of switching noise, causing zero-crossing events to be inconsistent. After the FIR filter is applied, the signal becomes smoother and more stable, as reflected by the improved quality of the commutation pulses and the motor speed response. Quantitatively, spectral analysis indicates that the dominant disturbance frequency in the detection signal is reduced from 317.23 Hz to 265.43 Hz following FIR filtering. This improvement directly enhances commutation stability, which is evident from the smoother motor speed response and the reduced fluctuations during the transient phase.

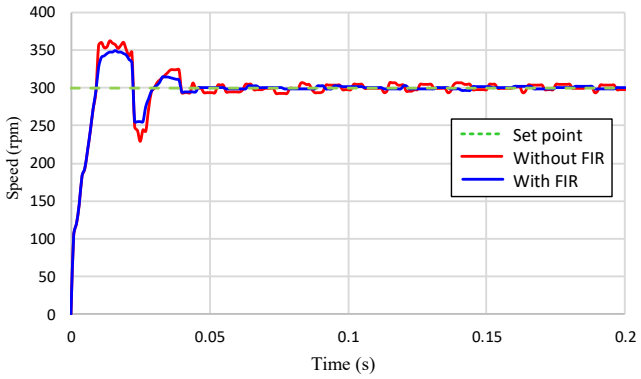

(a)

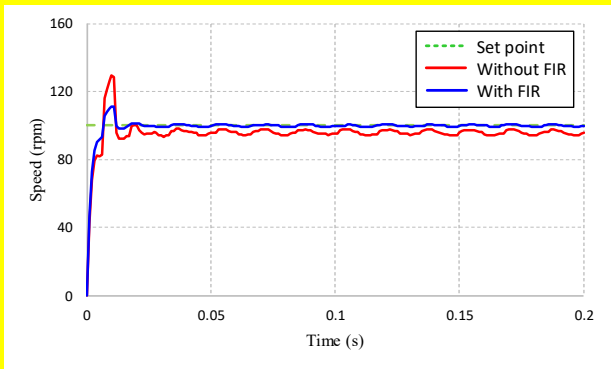

(b)

Figure 10. Comparison of BLDC Motor Speed Responses to the Set Point for Systems Without and With FIR Filtering Under Hardware Experimentation, (a) Set point 300 rpm; (b) Set point 100 rpm

Figure 10(a) and Figure 10(b) present the experimental comparison of the BLDC motor speed response to the reference set points under hardware implementation. In Fig. 10(a), corresponding to the 300 rpm set point, both systems exhibit a rapid rise toward the reference speed. However, the system without FIR filtering shows a larger overshoot, reaching approximately 350-360 rpm, along with more pronounced transient oscillations before stabilizing. These oscillations persist longer compared to the FIR-based system, indicating reduced damping and less accurate commutation timing. This behavior is primarily attributed to noise contamination in the Back-EMF signal, which introduces inaccuracies in zero-crossing detection and consequently leads to commutation timing errors. In contrast, the system employing FIR filtering exhibits a smaller overshoot and faster damping, achieving a smooth and stable convergence to the steady-state speed of approximately 300 rpm. This confirms that FIR filtering enhances signal integrity, resulting in improved commutation accuracy and system stability.

Similarly, Fig. 10(b), corresponding to the 100 rpm set point, highlights a more pronounced performance difference between the two systems, particularly at low-speed operation where the Back-EMF amplitude is inherently smaller and more susceptible to noise interference. The system without FIR filtering exhibits a higher overshoot, reaching approximately 120-130 rpm, and shows larger steady-state ripple compared to the FIR-based system. Conversely, the FIR-based system demonstrates reduced overshoot, faster settling time, and significantly lower steady-state speed fluctuations. The reduction in ripple amplitude indicates that the FIR filter effectively attenuates high-frequency noise and switching disturbances present in the Back-EMF signal.

The experimental results clearly demonstrate that the application of FIR filtering enhances the dynamic and steady-state performance of the sensorless BLDC motor. The FIR filter improves the reliability of zero-crossing detection, reduces commutation timing errors, and minimizes both transient oscillations and steady-state ripple. As a result, the FIR-based system achieves faster stabilization, improved speed accuracy, and superior operational stability compared to the unfiltered system. These improvements are particularly critical in low-speed operation, where signal integrity plays a crucial role in ensuring reliable sensorless commutation.

Table I. Comparison of the Dynamic Performance of the BLDC Motor Without and With FIR Filtering at Various Speed Set Points

Set Point (rpm)	Settling Time (ms)		Rise Time (ms)	
	Without FIR	With FIR	Without FIR	With FIR
100	3.2	2.4	5	4
200	4.3	2.8	4.2	4.3
300	4	3.3	4.5	4
400	4.4	3.8	10	9

Table I indicates that the application of FIR filtering consistently enhances the dynamic performance of the BLDC motor across all speed set points. In terms of settling time, the FIR-based system always achieves a shorter stabilization interval than the unfiltered system for example, at a set point of 100 rpm, the settling time is reduced from 3.2 ms to 2.4 ms, and at 300 rpm from 4.0 ms to 3.3 ms, demonstrating faster convergence to steady-state conditions. The rise time of the FIR-based system is also generally smaller or comparable, indicating a rapid initial response without

degrading transient behavior. Moreover, the steady-state speed achieved with FIR filtering is closer to the corresponding set point than that of the unfiltered system. These results suggest that the FIR filter not only improves transient stability but also enhances steady-state speed accuracy, thereby enabling the FIR-based system to exhibit faster, more stable, and more precise responses compared with the system without filtering.

4. Conclusions

This study demonstrates that the application of a Finite Impulse Response (FIR) digital filter to the Back-EMF detection signal effectively enhances the commutation performance of sensorless BLDC motors. Simulation results show that the dominant disturbance component in the Back-EMF signal is reduced from 347.6 Hz to 212.5 Hz, while hardware experiments indicate a reduction from 317.23 Hz to 265.43 Hz. This improvement in signal quality directly influences system dynamics, as evidenced by the reduction in settling time across all speed set points, for example, from 3.2 ms to 2.4 ms at 100 rpm and from 4.0 ms to 3.3 ms at 300 rpm. These results confirm that the FIR filter enhances the reliability of zero-crossing detection, accelerates convergence to steady-state conditions, and yields a smoother and more precise speed response. In future work, the proposed method will be extended to a closed-loop system with speed control, enabling a comprehensive evaluation of the impact of FIR filtering on control stability and overall performance.

5. References

[1] Y. Wu, Z. Deng, X. Wang, X. Ling and X. Cao, "Position Sensorless Control Based on Coordinate Transformation for Brushless DC Motor Drives," in IEEE Transactions on Power Electronics, vol. 25, no. 9, pp. 2365-2371, Sept. 2010, doi: 10.1109/TPEL.2010.2048126.

[2] C. -T. Lin, C. -W. Hung and C. -W. Liu, "Position Sensorless Control for Four-Switch Three-Phase Brushless DC Motor Drives," in IEEE Transactions on Power Electronics, vol. 23, no. 1, pp. 438-444, Jan. 2008, doi: 10.1109/TPEL.2007.911782.

[3] W. Li, J. Fang, H. Li and J. Tang, "Position Sensorless Control Without Phase Shifter for High-Speed BLDC Motors With Low Inductance and Nonideal Back EMF," in IEEE Transactions on Power Electronics, vol. 31, no. 2, pp. 1354-1366, Feb. 2016, doi: 10.1109/TPEL.2015.2413593.

[4] J. S. Park, K. -D. Lee, S. G. Lee and W. -H. Kim, "Unbalanced ZCP Compensation Method for Position Sensorless BLDC Motor," in IEEE Transactions on Power Electronics, vol. 34, no. 4, pp. 3020-3024, April 2019, doi: 10.1109/TPEL.2018.2868828.

[5] A. Sen and B. Singh, "Peak Current Detection Starting Based Position Sensorless Control of BLDC Motor Drive for PV Array Fed Irrigation Pump," in IEEE Transactions on Industry Applications, vol. 57, no. 3, pp. 2569-2577, May-June 2021, doi: 10.1109/TIA.2021.3066831.

[6] S. Chen, G. Liu and L. Zhu, "Sensorless Control Strategy of a 315 kW High-Speed BLDC Motor Based on a Speed-Independent Flux Linkage Function," in IEEE Transactions on Industrial Electronics, vol. 64, no. 11, pp. 8607-8617, Nov. 2017, doi: 10.1109/TIE.2017.2698373.

[7] S. Chen, W. Sun, K. Wang, G. Liu and L. Zhu, "Sensorless High-Precision Position Correction Strategy for a 100 kW@20 000 r/min BLDC Motor With Low Stator Inductance," in IEEE Transactions on Industrial Informatics, vol. 14, no. 10, pp. 4288-4299, Oct. 2018, doi: 10.1109/TII.2018.2793947

[8] M. Mohammed, D. Ishak and K. Hammadi, "Improved speed operation of sensorless BLDC motor drives using IIR digital filter," 2010 IEEE International Conference on Power and Energy, Kuala Lumpur, Malaysia, 2010, pp. 759-764, doi: 10.1109/PECON.2010.5697682.

[9] C.W. Tsai, C.H. Huang, and C.L. Lin, “Structure-specified IIR filter and control design using real structured genetic algorithm,” Applied Soft Computing, vol. 9, no. 4, pp. 1285–1295, 2009, doi: 10.1016/j.asoc.2009.04.001.

[10] A. A. Obed, A. L. Saleh, and A. K. Kadhim, “Speed performance evaluation of BLDC motor based on dynamic wavelet neural network and PSO algorithm,” Int. J. Power Electronics and Drive Systems (IJPEDS), vol. 10, no. 4, pp. 1742–1750, Dec. 2019, doi: 10.11591/ijpeds.v10.i4.pp1742-1750.

[11] C. Shrutika, S. Matani, S. Chaudhuri, A. Gupta, S. Gupta and N. Singh, "Back-EMF estimation based sensorless control of Brushless DC motor," 2021 1st International Conference on Power Electronics and Energy (ICPEE), Bhubaneswar, India, 2021, pp. 1-6, doi: 10.1109/ICPEE50452.2021.9358657.

[12] A. Attar, J. Bouchnaif, and K. Grari, “Control of brushless DC motors using sensorless back-EMF integration method,” Materials Today: Proceedings, vol. 45, pt. 8, pp. 7438–7443, 2021, doi: 10.1016/j.matpr.2021.01.861.

[13] Yao, X., Ma, C., Zhao, J. and De Belie, F. (2020), Rapid estimation and compensation method of commutation error caused by Hall sensor installation error for BLDC motors. IET Electric Power Applications, 14: 337-347.doi: 10.1049/ietepa.2018.5941

[14] Alanis, Alma Y., Gustavo Munoz-Gomez, and Jorge Rivera. 2020. "Nested High Order Sliding Mode Controller with Back-EMF Sliding Mode Observer for a Brushless Direct Current Motor" Electronics 9, no. 6: 1041. https://doi.org/10.3390/electronics906104.

[15] Maurice Bellanger, Benjamin A. Engel, "Finite Impulse Response (FIR) Filters," in Digital Signal Processing: Theory and Practice , Wiley, 2024, pp.89-122, doi: 10.1002/9781394182695.ch5.

[16] Bellanger, M. (2024). Finite Impulse Response (FIR) Filters . In Digital Signal Processing (eds M. Bellanger and B. Engel). https://doi.org/10.1002/9781394182695.ch5

[17] Nerma, M. H. M., Elfaki, A. O., Bushnag, A., & Alnemari, M. "An Innovative Finite Impulse Response Filter Design Using a Combination of L1/L2 Regularization to Improve Sparsity and Smoothness" Electronics 14, no. 22: 4386., 2025, https://doi.org/10.3390/electronics14224386

[18] M. Bellanger and B. Engel, “Finite Impulse Response (FIR) Filters,” in Digital Signal Processing. Hoboken, NJ, USA: Wiley, 2024. doi: 10.1002/9781394182695.ch5.

[19] M. F. Karakaş and F. Latifoğlu, “Finite impulse response filter design using squirrel search algorithm,” in Proc. 2020 Medical Technologies Congress (TIPTEKNO), Antalya, Turkey, Nov. 2020, pp. 1–4. doi: 10.1109/TIPTEKNO50054.2020.9299250.